

# AN INTELLIGENT PERSONAL NAVIGATOR INTEGRATING GNSS, RFID AND INS FOR CONTINUOUS POSITION DETERMINATION

*Um navegador pessoal inteligente integrando GNSS, RFID e INS para  
determinação contínua da posição.*

G. RETSCHER  
Q. FU

Institute of Geodesy and Geophysics  
Vienna University of Technology, Austria  
gretsch@pop.tuwien.ac.at, fu@mail.zserv.tuwien.ac.at

## ABSTRACT

Most of the developed pedestrian navigators rely on the use of satellite positioning (GNSS), sometimes also in combination with other sensors and positioning methods. In the project “Ubiquitous Cartography for Pedestrian Navigation” (UCPNAVI) we have integrated active Radio Frequency Identification (RFID) in combination with GNSS and Inertial Navigation Systems (INS) for continuous positioning. RFID can be employed in areas where no satellite positioning is possible due to obstructions, e.g. in urban canyons and indoor environments. In RFID positioning the location estimation is based on Received Signal Strength Indication (RSSI) which is a measurement of the power present in a received radio signal. The receiver can compute its position using various methods based on RSSI. In total, three different methods have been developed and investigated, i.e., cell-based positioning, trilateration and RFID location fingerprinting. These methods can be employed depending on the density of the RFID tags in the surrounding environment providing different levels of positioning accuracies. By integrating the three methods for positioning into an intelligent software package and developing a knowledge-based system it is possible to determine the pedestrian position automatically and ubiquitously. The concept of the intelligent software package is presented and described in the paper. For improvement of the positioning accuracy of cell-based positioning a modification has been developed, the so-called time-based Cell of Origin (CoO) positioning method. This method uses also the measured RSSI above a certain threshold which is measured only if the user is located very close to the RFID tag. The test results showed that the accuracy of positioning using time-based CoO is in the range of 1.30 m. For continuous

positioning of the pedestrian user, a low-cost INS is employed in addition. Since the INS components produce small measurement errors that accumulate over time and cause drift errors, the positions determined by RFID would be needed regularly for update. For the combined positioning of RFID and INS a time-varying Kalman filter is employed. The approach is tested in indoor environment in an office building of our university. For the combined positioning, an accuracy of around 1.00 m for continuous position determination is achieved. The new approach and the test results are also described in this paper.

**Keywords:** GPS/INS; Integration; Navigation; Mobile; Multi-Sensor.

## 1. INTRODUCTION

Personal navigation and guidance services usually rely on GNSS positioning and therefore their use is limited to open areas where adequate satellite signals can be received. If the user moves in obstructed urban environment or indoors, alternative location methods are required to be able to locate the user continuously. In our approach GNSS positioning is combined with a MEMS-based Inertial Measurement Unit for continuous position determination. In addition, Radio Frequency Identification (RFID) Location Methods are employed to replace GNSS in obstructed areas. RFID can also be used for positioning, because the location estimation can be based on signal strength measurements (i.e., received signal strength indication RSSI) which is a measurement of the power present in a received radio signal. Then the mobile receiver can compute its position using various methods based on RSSI.

Totally, three different methods have been developed and investigated, i.e., cell-based positioning, trilateration using ranges to the surrounding RFID transponders (so-called RFID tags) deduced from RSSI measurements and RFID location fingerprinting. In most common RFID applications positioning is performed using the cell-based positioning principle. In this case, RFID tags can be installed at active landmarks with known location in the surroundings. Then the user is carrying an RFID reader and is positioned using Cell of Origin (CoO). The achievable positioning accuracy thereby depends on the size of the cell defined by the maximum read range of the signal. Using long range active RFID this read range can be quite large, i.e., up to 40 to 80 m. Higher positioning accuracies can be achieved using a modification of cell-based positioning which is called time-based CoO. In this approach, the location of the RFID tag is used to describe the current position of the user only if the received signal strength from the tag is above a certain threshold. The maximum in signal strength usually only appears when the user is currently located very close to the tag's position. If more than one maximum in signal strength is detected at different times, then the mean value for the time epoch is taken when the user is nearest to the tag. This developed approach provides positioning accuracies on the one meter level and will be introduced in this paper.

Apart from cell-based positioning also trilateration and location fingerprinting can be employed when the RSSI of more than two RFID tags can be read at the same time. Positioning accuracies on the one to several metre level can be achieved for a continuously moving user.

GNSS and RFID as well are then integrated with INS positioning for continuous position determination of a pedestrian. INS measurements would be utilized to calculate the trajectory of the user based on the method of strap down mechanization. Since the INS components produce small measurement errors that accumulate over time and cause drift errors, the positions determined by RFID or GNSS would be needed regularly to eliminate and reduce these errors. All observations are then integrated in a Kalman filter to estimate the user's position and velocity. By integrating the above mentioned measurements into an intelligent software package the developed personal navigator will enable to determine the mobile user's position continuously, automatically and ubiquitously.

This paper is organized as follows: first of all, the different RFID positioning methods are briefly described in section 2 followed by a detailed description of continuous positioning using RFID and INS in section 3. Indoor positioning test results are presented in section 4. In section 5, the concept for the development of an intelligent software package is introduced followed by concluding remarks in section 6.

## **2. RFID FOR POSITIONING OF A PEDESTRIAN**

In RFID positioning of a pedestrian, the location estimation is based on RSSI which is a measurement of the power present in a received radio signal. The receiver can compute its position using various methods based on RSSI. In total, three different methods have been employed, i.e., cell-based positioning, trilateration using ranges to the surrounding RFID tags deduced from received signal strength measurements and RFID location fingerprinting (Fu, 2008). These technologies can be employed depending on the density of the RFID transponders (so-called tags) in the surrounding environment. For positioning with RFID either readers or tags can be placed at known location in the surrounding environment. We have chosen a low-cost concept where the less expensive tags are deployed in the surrounding environment at active landmarks (i.e., known location) or at regular distances. The mobile user is carrying a reader in form of a PC-card, which can be plugged into the mobile device (e.g. a pocket PC or laptop).

The most straightforward method is cell-based positioning. The maximum range of the RFID tag defines a cell of circular shape in which a data exchange between the tag and the reader is possible. Several tags located in the smart environment can overlap and define certain cells with a radius equal the read range. The accuracy of position determination is defined by the cell size. Using active RFID tags the positioning accuracy therefore ranges between a few meters up to

tens of meters. However, the accuracy could be improved by using the so-called time-based CoO. In time-based CoO two improvements of the standard cell-based positioning have been made to get a higher positioning accuracy. First of all, a threshold value is set to reduce the size of the cell. Secondly, the mean value of the corresponding time is calculated for all signal strength measurements above the threshold (compare Figure 3). As a result, the positioning accuracy is improved. The RFID time for each detected ID is the mean value of the corresponding time. The location determined in this way ensures that the calculated position is closest to the true position of the RFID tag. The approach takes the fact into account that the received signal strength is highly variable in indoor environments with a large number of obstacles and moving objects which affect the propagation of the RFID signals.

For verification of the RFID time-based CoO measurements a tool was developed under the environment of Microsoft Visual Studio 2008. If the user passes by an RFID tag a marker can be set in the program by a simple mouse click capturing the system time. This is used as an indication for the user currently being nearest to the true location of the RFID tag. The verification tool is called "time data capture tool". The known RFID tag coordinates are regarded as true positions at this point of time. The location determined by the integration of RFID and INS at the corresponding point of time is the estimated position. The differences between these two positions are the estimated errors.

As an alternative to time-based CoO, trilateration and location fingerprinting have been investigated. Trilateration can be employed if the ranges to several tags in the surrounding environment can be determined. Then these ranges are used for intersection. The range from the antenna of the reader to the antenna of the tag is deduced from the conversion of signal strength into distances. Strategies for the conversion of the signal strength measurements into distances are distinguished between indoor and urban outdoor environment. It was found that a simple polynomial relationship between the signal strength and the range provides reasonable results (see Fu and Retscher, 2009b). The highest positioning accuracies can be obtained with location fingerprinting. In case of RFID location fingerprinting (Kaemarungsi, 2005; Retscher et al., 2007), RSSI is measured in a training phase at known locations and stored in a database. In the positioning phase, these measurements are used together with the current measurements to obtain the current location of the user. Location fingerprinting, however, is more costly and complicated in comparison to cell-based positioning and trilateration. For this method different advanced approaches have been developed and tested (see Fu, 2008). For the creation of the database in RFID location fingerprinting interpolation methods can be used, in order to achieve a further improvement of the positioning accuracy.

To test the different methods experiments have been conducted in a test bed near and in the university building of the Vienna University of Technology in

downtown Vienna. The conducted experiments (see e.g. Fu, 2008; Fu and Retscher, 2009b) showed that these approaches are suitable to navigate the user with different positioning accuracies, i.e., lower positioning accuracies on the several meter level in outdoor environment using cell-based positioning and higher positioning accuracies on the one meter level in indoor environments with trilateration and fingerprinting.

### 3. CONTINUOUS POSITIONING WITH RFID AND INS

The RFID positioning is restricted, however, to areas where at least one RFID signal can be detected. If there is lack of coverage of signals of the RFID tags, the RFID reader will lose its capability for continuous positioning. In order to overcome these shortages, we have integrated a low-cost Inertial Navigation System (INS) in addition. In the following, first of all the determination of trajectories using an INS is explained and then the fusion of RFID and INS is discussed and presented. The approach is verified by field tests and the results of the experiment are presented in the next section.

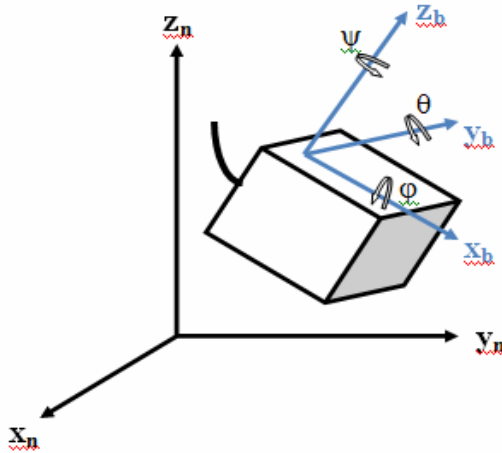
#### 3.1 Trajectory Determination with Low-cost Inertial Navigation System (INS)

Generally, inertial systems are categorized in two groups (Lawrence, 1998; Gabaglio, 2002): gimbals and strapdown INS. The gimbaled systems are heavy and large. Hence, they are unsuitable for pedestrian navigation. In contrast to gimbaled systems a strapdown system has advances in sensor development (Barbour, 2001) in terms of size, precision and cost, as well as in computation capabilities of processor and can, therefore, be utilized for pedestrian navigation. The term “strapdown” can be dated back to the technique that modern systems have removed most of the mechanical complexity of platform systems by having the sensors attached rigidly, or “strapped down”, to the body of the host vehicle (Titterton and Weston, 2005).

Normally, an INS is composed of three gyroscopes and three accelerometers. All the sensors are mounted orthogonal. They are used to measure the angular rate and to capture the acceleration in one of the three directions. It is to be noted that the measurements are in the right handed Cartesian coordinate system. This coordinate system is body-fixed to the device and is defined as the body frame. The body frame changes with respect to the navigation frame. The relationship between these two frames can be described by attitude parameters which are defined as the orientations in space of the INS body frame (see Figure 1).

Usually, the attitude is numerically represented by a 3x3 matrix  $\mathbf{R}$  that is an orthogonal endomorphism. Generally, the attitude can be parameterized in two ways: using Quaternions and using Euler angles. Euler angles  $(\phi, \theta, \psi)$  are equivalent to “roll, pitch and yaw” (see Figure 1). Quaternions  $\mathbf{q}_0, \mathbf{q}_1, \mathbf{q}_2, \mathbf{q}_3$  are an efficient, non-singular description of 3-D orientation and have advantages from a numerical and computational point of view (Shuster 1993).

Figure 1 - The INS body frame (x,y,z) and the navigation frame (X,Y,Z)



INS obtains measurements for the rate of turn using a gyroscope and acceleration using an accelerometer. These measurements need to be integrated over time to obtain orientation changes and velocity measurements. Then the current position could be derived by integrating the obtained orientation changes and velocity measurements over time if the start position could be given for the integration. The strapdown mechanization in our approach uses the orientation data from the INS (unit quaternions  $\mathbf{q}_0, \mathbf{q}_1, \mathbf{q}_2, \mathbf{q}_3$  or Euler parameters  $\phi, \theta, \psi$ ) and the calibration data (rate of turn from the gyroscope  $\mathbf{gyr}_{x_b}, \mathbf{gyr}_{y_b}, \mathbf{gyr}_{z_b}$  and acceleration from the accelerometer  $\mathbf{acc}_x, \mathbf{acc}_y, \mathbf{acc}_z$ ) to obtain the trajectory of the INS. This process is divided into two steps. Firstly, the input data are used to calculate the free acceleration  $\mathbf{acc}_{x_b}, \mathbf{acc}_{y_b}, \mathbf{acc}_{z_b}$  and the rotation matrix  $\mathbf{R}_{nb}$ , whereby, in the free acceleration the gravity and centrifugal force are not included, and the rotation matrix is used for the transformation between the body frame  $\mathbf{b}$  and the navigation frame  $\mathbf{n}$ . In the second step, the position of user  $\mathbf{p}_{x_n}, \mathbf{p}_{y_n}, \mathbf{p}_{z_n}$  in the navigation frame is computed by integrating acceleration and velocity over time.

The Euler angles  $\phi_{nb}, \theta_{nb}$  and  $\psi_{nb}$  are calculated by using the quaternions  $\mathbf{q}_0, \mathbf{q}_1, \mathbf{q}_2, \mathbf{q}_3$  which can be obtained from the sensor directly:

$$\begin{bmatrix} \phi_{nb} \\ \theta_{nb} \\ \psi_{nb} \end{bmatrix} = \begin{bmatrix} \mathbf{atan2}(2\mathbf{q}_2\mathbf{q}_3 + 2\mathbf{q}_0\mathbf{q}_1, 2\mathbf{q}_0^2 + 2\mathbf{q}_3^2 - 1) \\ -\mathbf{asin}(2\mathbf{q}_1\mathbf{q}_3 - 2\mathbf{q}_0\mathbf{q}_2) \\ \mathbf{atan2}(2\mathbf{q}_1\mathbf{q}_2 + 2\mathbf{q}_0\mathbf{q}_3, 2\mathbf{q}_0^2 + 2\mathbf{q}_1^2 - 1) \end{bmatrix} \cdot \frac{\pi}{180} \quad (1)$$

After that the orientation angles  $\phi$ ,  $\theta$  and  $\psi$  regarding the navigation frame of the sensor can be obtained by integrating the rate of turn  $\mathbf{gyr}_{x\_b}$ ,  $\mathbf{gyr}_{y\_b}$ ,  $\mathbf{gyr}_{z\_b}$  over the time:

$$\begin{bmatrix} \phi \\ \theta \\ \psi \end{bmatrix} = \begin{bmatrix} \phi_{nb} \\ \theta_{nb} \\ \psi_{nb} \end{bmatrix} + \begin{bmatrix} 1 & \frac{\sin\phi_{nb} \sin\theta_{nb}}{\cos\theta_{nb}} & \frac{\cos\phi_{nb} \sin\theta_{nb}}{\cos\theta_{nb}} \\ 0 & \cos\theta_{nb} & -\sin\phi_{nb} \\ 0 & \frac{\sin\phi_{nb}}{\cos\theta_{nb}} & \frac{\cos\phi_{nb}}{\cos\theta_{nb}} \end{bmatrix} \cdot \begin{bmatrix} \mathbf{gyr}_{x\_b} - \mathbf{gyr}_{x0\_b} \\ \mathbf{gyr}_{y\_b} - \mathbf{gyr}_{y0\_b} \\ \mathbf{gyr}_{z\_b} - \mathbf{gyr}_{z0\_b} \end{bmatrix} \cdot dt \quad (2)$$

Then the rotation matrix  $\mathbf{R}_{nb}$  from the body frame  $\mathbf{b}$  to the navigation frame  $\mathbf{n}$  can be computed:

$$\begin{aligned} \mathbf{R}_{nb} &= \mathbf{R}_{\psi}^z \cdot \mathbf{R}_{\theta}^y \cdot \mathbf{R}_{\phi}^x \\ &= \begin{bmatrix} \cos\theta\cos\psi & \sin\phi\sin\theta\cos\psi - \cos\phi\sin\psi & \cos\phi\sin\theta\cos\psi + \sin\phi\sin\psi \\ \cos\theta\sin\psi & \sin\phi\sin\theta\sin\psi + \cos\phi\cos\psi & \cos\phi\sin\theta\sin\psi - \sin\phi\cos\psi \\ -\sin\theta & \sin\phi\cos\theta & \cos\phi\cos\theta \end{bmatrix} \end{aligned} \quad (3)$$

Note that the transpose of the rotation matrix  $\mathbf{R}_{nb}$  is equivalent to the rotation matrix  $\mathbf{R}_{bn}$  from the navigation frame  $\mathbf{n}$  to the body frame  $\mathbf{b}$ .

Now the free acceleration will be deduced. The free acceleration here is the second derivative of the position that does not include the acceleration due to gravity and centrifugal force in contrast to the original measured linear acceleration. This is inherent to all accelerometers (Xsens, 2007). Therefore, the gravity and centrifugal force must be subtracted from the measured linear acceleration, so that the free acceleration could be obtained.

$$\begin{bmatrix} \mathbf{acc}_{x\_b} \\ \mathbf{acc}_{y\_b} \\ \mathbf{acc}_{z\_b} \end{bmatrix} = \begin{bmatrix} \mathbf{acc}_x \\ \mathbf{acc}_y \\ \mathbf{acc}_z \end{bmatrix} + \begin{bmatrix} \mathbf{gyr}_{x\_b} - \mathbf{gyr}_{x0\_b} \\ \mathbf{gyr}_{y\_b} - \mathbf{gyr}_{y0\_b} \\ \mathbf{gyr}_{z\_b} - \mathbf{gyr}_{z0\_b} \end{bmatrix} \times \begin{bmatrix} \mathbf{v}_{x\_b} \\ \mathbf{v}_{y\_b} \\ \mathbf{v}_{z\_b} \end{bmatrix} - \underbrace{(\mathbf{R}_{nb})^T}_{\mathbf{R}_{bn}} \cdot \begin{bmatrix} \mathbf{acc}_{x0} \\ \mathbf{acc}_{y0} \\ \mathbf{acc}_{z0} \end{bmatrix} \quad (4)$$

Concerning that there are drifts in the measurements of rate of turn and acceleration, one more measurement was carried out by keeping the Xsens device

unmoved for a short time period, in order to find out the drifts. These drifts ( $\mathbf{gyr}_{x0\_b}$ ,  $\mathbf{gyr}_{y0\_b}$ ,  $\mathbf{gyr}_{z0\_b}$  and  $\mathbf{acc}_{x0}$ ,  $\mathbf{acc}_{y0}$ ,  $\mathbf{acc}_{z0}$ ) are subtracted from the measurements while the INS sensor was moved (see equation 4).

After the free acceleration and rotation matrix have been calculated from the original measured orientation and calibration data, they would be integrated over time to obtain the orientation changes and velocity measurements. Then the current position could be derived by integrating the obtained orientation changes and velocity measurements over time and using the position from the last calculation. These processes occur in the second step of the determination of the trajectory using INS.

The current user position must also be transformed into the navigation frame  $\mathbf{n}$ . The first integration of the accelerations  $\mathbf{acc}_{x\_b}$ ,  $\mathbf{acc}_{y\_b}$ ,  $\mathbf{acc}_{z\_b}$  leads to the velocities  $\mathbf{v}_{x\_b}$ ,  $\mathbf{v}_{y\_b}$ ,  $\mathbf{v}_{z\_b}$  in the body frame  $\mathbf{b}$ . Then the velocities  $\mathbf{v}_{x\_n}$ ,  $\mathbf{v}_{y\_n}$ ,  $\mathbf{v}_{z\_n}$  in the navigation frame  $\mathbf{n}$  can be obtained. The 3-D coordinates  $\mathbf{p}_{x\_b}$ ,  $\mathbf{p}_{y\_b}$ ,  $\mathbf{p}_{z\_b}$  in the body frame  $\mathbf{b}$  can be calculated by integrating the above obtained velocities over time. Then the user position  $\mathbf{p}_{x\_n}$ ,  $\mathbf{p}_{y\_n}$ ,  $\mathbf{p}_{z\_n}$  in the navigation frame  $\mathbf{n}$  can be obtained. This process has to be done recursively starting from the position from the last calculation.

### 3.2 Fusion of RFID and INS Positioning

In our attempt presented in this paper RFID time-based CoO (compare section 2) is combined with the INS positioning. Then the absolute positioning with RFID can be used to correct the drift of the INS which is caused by the accumulation of errors of the sensors. For the integration of INS with either GNSS or RFID positions usually a Kalman Filter is employed. In the algorithm, the strapdown INS local geographic navigation frame mechanization (Titterton and Weston, 2005) is combined with the three-axes inertial error model (Brown and Hwang, 1997) and the RFID time-based CoO method to produce accurate and continuous positioning estimations. A basic 9-state dynamic model is used as the RFID/INS Kalman Filter model. In the model, the state vector  $\mathbf{x}$  contains three position errors, three velocity errors and three Euler angle errors. Using such a Kalman Filter a meaningful integration of INS with RFID can be performed (Fu and Retscher, 2009a).

In our approach, we used a so-called time-varying Kalman filter developed in Matlab programming environment which is a generalization of the steady-state filter for time-varying systems with nonstationary noise covariance and is given by the recursions.

The continuous-time state equation of the time-varying Kalman filter is given by:



$$\underbrace{\begin{bmatrix} \dot{\mathbf{p}}_x \\ \dot{\mathbf{p}}_y \\ \dot{\mathbf{v}}_x \\ \dot{\mathbf{v}}_y \\ \dot{\Psi} \end{bmatrix}_t}_{\mathbf{x}(t) \text{ state vector at time } t} = \underbrace{\begin{bmatrix} 0 & 0 & 1 & 0 & 0 \\ 0 & 0 & 0 & 1 & 0 \\ 0 & 0 & 0 & 0 & 0 \\ 0 & 0 & 0 & 0 & 0 \\ 0 & 0 & 0 & 0 & 0 \end{bmatrix}}_{\mathbf{A}^* \text{ state transition matrix}} \cdot \underbrace{\begin{bmatrix} \mathbf{p}_x \\ \mathbf{p}_y \\ \mathbf{v}_x \\ \mathbf{v}_y \\ \Psi \end{bmatrix}_t}_{\mathbf{x}(t) \text{ state vector at time } t} + \underbrace{\begin{bmatrix} 0 & 0 & 0 \\ 0 & 0 & 0 \\ \cos \Psi & -\sin \Psi & 0 \\ \sin \Psi & \cos \Psi & 0 \\ 0 & 0 & 1 \end{bmatrix}}_{\mathbf{B}^* \text{ input matrix}} \cdot \underbrace{\begin{bmatrix} \text{acc}_{x,b} \\ \text{acc}_{y,b} \\ \text{gyr}_{z,b} \end{bmatrix}_t}_{\mathbf{u}(t) \text{ input vector}} + \underbrace{\begin{bmatrix} 1 & 0 \\ 0 & 1 \\ 0 & 0 \\ 0 & 0 \\ 0 & 0 \end{bmatrix}}_{\mathbf{S}^* \text{ noise matrix}} \cdot \underbrace{\mathbf{w}^*(t)}_{\text{gaussian process noise with covariance } Q_{w^*w^*} \text{ at time } t} \tag{5}$$

Equation 5 can be transferred into a discrete-time state equation:

$$\underbrace{\begin{bmatrix} \mathbf{p}_x \\ \mathbf{p}_y \\ \mathbf{v}_x \\ \mathbf{v}_y \\ \Psi \end{bmatrix}_{k+1}}_{\mathbf{x}[k+1] \text{ state vector at time } k+1} = \underbrace{\begin{bmatrix} 1 & 0 & \Delta t & 0 & 0 \\ 0 & 1 & 0 & \Delta t & 0 \\ 0 & 0 & 1 & 0 & 0 \\ 0 & 0 & 0 & 1 & 0 \\ 0 & 0 & 0 & 0 & 1 \end{bmatrix}}_{\mathbf{A} \text{ state transition n matrix}} \cdot \underbrace{\begin{bmatrix} \mathbf{p}_x \\ \mathbf{p}_y \\ \mathbf{v}_x \\ \mathbf{v}_y \\ \Psi \end{bmatrix}_k}_{\mathbf{x}[k] \text{ state vector at time } k} + \underbrace{\begin{bmatrix} \frac{1}{2} \Delta t^2 \cdot \cos \Psi & -\frac{1}{2} \Delta t^2 \cdot \sin \Psi & 0 \\ \frac{1}{2} \Delta t^2 \cdot \sin \Psi & \frac{1}{2} \Delta t^2 \cdot \cos \Psi & 0 \\ \Delta t \cdot \cos \Psi & -\Delta t \cdot \sin \Psi & 0 \\ \Delta t \cdot \sin \Psi & \Delta t \cdot \cos \Psi & 0 \\ 0 & 0 & \Delta t \end{bmatrix}}_{\mathbf{B} \text{ input matrix}} \cdot \underbrace{\begin{bmatrix} \text{acc}_{x,b} \\ \text{acc}_{y,b} \\ \text{gyr}_{z,b} \end{bmatrix}_k}_{\mathbf{u}[k] \text{ input vect or}} + \underbrace{\begin{bmatrix} \Delta t & 0 \\ 0 & \Delta t \\ 0 & 0 \\ 0 & 0 \\ 0 & 0 \end{bmatrix}}_{\mathbf{S} \text{ noise matrix}} \cdot \underbrace{\begin{bmatrix} \mathbf{w}_{v_x} \\ \mathbf{w}_{v_y} \end{bmatrix}_k}_{\mathbf{w}[k] \text{ gaussian process noise with covariance } Q_{ww} \text{ at time } k} \tag{6}$$

The measurement equation is:

$$\underbrace{\begin{bmatrix} p_{x\_n} \\ p_{y\_n} \end{bmatrix}}_{\mathbf{y}_v[k]} = \underbrace{\begin{bmatrix} 1 & 0 & 0 & 0 & 0 \\ 0 & 1 & 0 & 0 & 0 \end{bmatrix}}_{\mathbf{C}} \cdot \underbrace{\begin{bmatrix} p_{x\_n\_kf} \\ p_{y\_n\_kf} \\ v_{x\_n\_kf} \\ v_{y\_n\_kf} \\ \psi_{kf} \end{bmatrix}}_{\mathbf{x}[k]} + \underbrace{\mathbf{v}[k]}_{\text{measurement noise with covariance R at time k}} \tag{7}$$

observation vector  
with noise  $v$   
at time  $k$

observation matrix

state vector  
at time  $k$

The system noise covariance matrix  $\mathbf{Q}$  is:

$$\mathbf{Q}_{\mathbf{w}\mathbf{w}} = \begin{bmatrix} \sigma_{v_{x\_b}}^2 & 0 \\ 0 & \sigma_{v_{y\_b}}^2 \end{bmatrix}, \quad \mathbf{Q}_{\mathbf{u}\mathbf{u}} = \begin{bmatrix} \sigma_{acc_{x\_b}}^2 & 0 & 0 \\ 0 & \sigma_{acc_{y\_b}}^2 & 0 \\ 0 & 0 & \sigma_{gyr_{z\_b}}^2 \end{bmatrix} \tag{8}$$

where  $\sigma_{v_{x\_b}} = 2$  is the velocity noise in the x axis in [m/s],  
 $\sigma_{v_{y\_b}} = 2$  is the velocity noise in the y-axis in [m/s],  
 $\sigma_{acc_{x\_b}} = 0.012$  is the accelerometer noise in the x-axis in [m/s<sup>2</sup>],  
 $\sigma_{acc_{y\_b}} = 0.012$  is the accelerometer noise in the y-axis in [m/s<sup>2</sup>] and  
 $\sigma_{gyr_{z\_b}} = 0.007$  is the gyroscope noise in the z-axis in [rad]  
 with the **bias** = 0.012 [m/s<sup>2</sup>] and **drift** = 0.007 [rad/s] as given by the sensor manufacturer.

The observation error covariance matrix  $\mathbf{R}$  is:

$$\mathbf{R} = \begin{bmatrix} \sigma_{p_{x\_n}}^2 & 0 \\ 0 & \sigma_{p_{y\_n}}^2 \end{bmatrix} \tag{9}$$

where  $\sigma_{p_{x\_n}} \geq 1$  [m] and  $\sigma_{p_{y\_n}} \geq 1$  [m] ( $\mathbf{R}$  matrix for RFID is indicated by  $\mathbf{R}_{\text{RFID}}$ ),

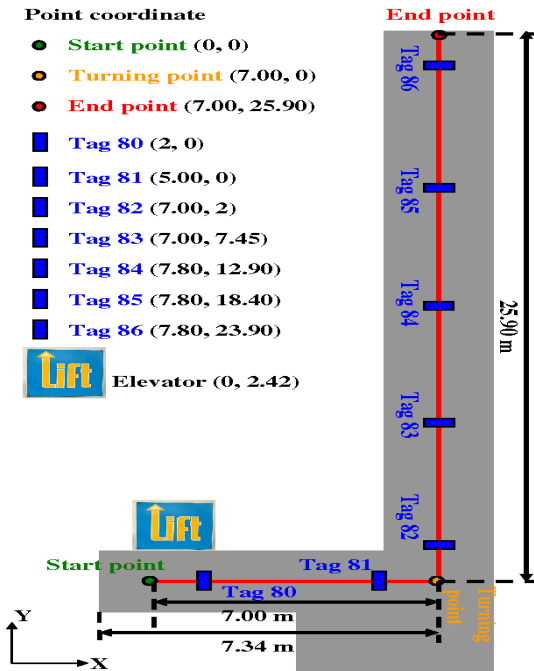
$$\sigma_{p_{x,n}} = 0 \text{ [m]} \text{ and } \sigma_{p_{y,n}} = 0 \text{ [m]} \text{ (R matrix for INS is indicated by } \mathbf{R}_{INS}\text{).}$$

Using new measurements the state vector can be recursively updated in the Kalman filter process.

#### 4. INDOOR POSITIONING TEST

This section presents the integration of RFID and low-cost INS for continuous positioning in an indoor environment. In the project, a low-cost INS from Xsens, the MTi, has been employed. For calculating the positions from the measured data of the sensor the strapdown mechanization is used. Furthermore, a time-varying Kalman filter is employed to correct the position and acceleration resulted from the strapdown mechanization. RFID time-based CoO positioning is utilized to determine the current position of the user, when the RFID reader detects a signal from an RFID tag in the surrounding environment. This determined position will be needed to update and correct the trajectory calculated by the INS, since the INS components produce small measurement errors that accumulate over time and cause drift errors.

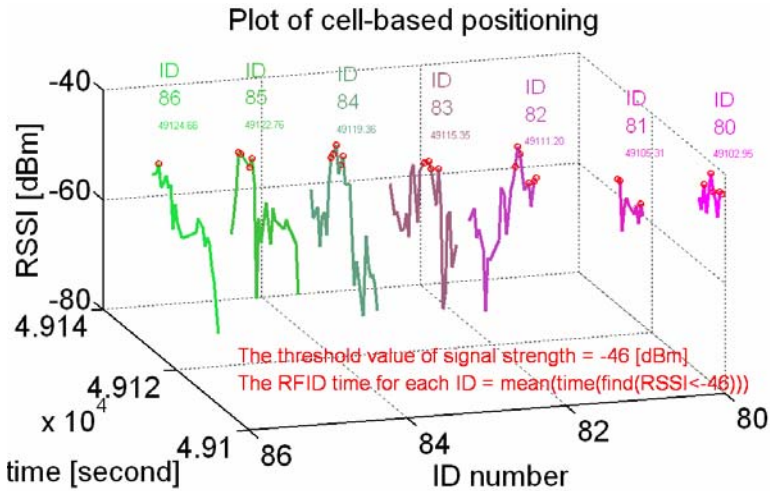
Figure 2 - Indoor positioning test environment.



The indoor positioning test was conducted on the 3<sup>rd</sup> floor in an office building of the Vienna University of Technology (see Figure 2). The trajectory starts in front of the elevator (referred to as “Lift” in Figure 2) and leads to a general teaching room along a corridor around the corner. The route is totally 32.9 m long and can be divided into two sections which are rectangular to each other. The second part of the route runs along the middle line of the corridor and has a length of 25.9 m. The reference trajectory is shown as solid line in Figure 2. In total, seven RFID tags were mounted in the test bed evenly distributed. Tags were suspended from the ceiling in a height of 2.0 m above the ground.

In this experiment cell-based positioning was employed for RFID positioning. Figure 3 shows the signal reception using cell-based positioning including the information of the RSSI, the time the tag was detected, and the ID of the tag. Each tag is identified by its presence or absence and the measured signal strength RSSI. As indicated by the circles, RSSI measurements which were higher than the threshold value of -46 dBm are selected for time-based CoO.

Figure 3 - Signal reception using cell-based positioning.



The position determined using RFID cell-based positioning was utilized in order to update the trajectory calculated by using the measurements of the INS. The Xsens MTi sensor bandwidth was 100 Hz. Additionally, a Kalman Filter is used to correct the position and velocity dynamics of the INS sensor. Figure 4 shows the filter result of the INS trajectory. The dashed line represents the measured response

by using the strapdown mechanization without filtering, while the solid line represents the result of the positions filtered by the Kalman Filter. The error in position increased over time with a maximum error in y-direction of around 2.50 m and a maximum error in x-direction of around 15.00 m. However, the error could be significantly reduced using the Kalman Filter. Figure 4 denotes that all points are positioned with a maximum radial deviation of 2.65 m and with a mean radial deviation of around 0.90 m. It can be seen that the mean radial deviation plus standard deviation is in the range of 1-2 m. Therefore, an accuracy in this range for continuous positioning in indoor environments can be achieved.

Figure 4 - Filter result of the INS trajectory.

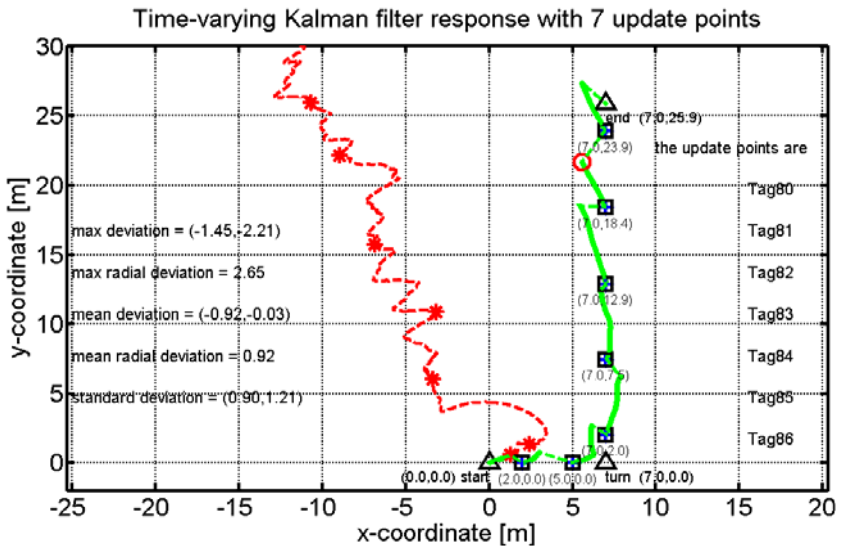


Table 1 includes the estimated error of positioning using the integrated system. It can be seen that the maximum error in x-direction is 0.41 m, while the maximum error in y-direction is 1.04 m. The maximum error in position is 1.05 m.

In Table 1,  $dx_f$  is the deviation between the filtered and true location of the tags along the x-axis,  $dy_f$  is the deviation between the filtered and true location of the tags along the y-axis and  $dr_f$  is the radial deviation between the filtered and true location of the tags.

Table 1 - Estimated positioning error of integrated system.

Tag Nr.	$dx_r$ [m]	$dy_r$ [m]	$dr_r$ [m]
Tag80	0.17	0.01	0.17
Tag81	0.30	-0.08	0.31
Tag82	0.41	0.48	0.63
Tag83	0.29	0.47	0.56
Tag84	0.04	-0.22	0.22
Tag85	0.09	-0.57	0.58
Tag86	-0.12	1.04	1.05
max			1.05
min			0.17
mean			0.50
std			0.30

The experiment showed that the determination of the trajectory using an integration of RFID and the INS achieved an accuracy of around 1.00 m in two directions on the x-y plan. Furthermore, the maximal error of the positioning was 1.40 m along the x-axis and 1.20 m along the y-axis. This accuracy is suitable for most positioning applications in indoor environments.

## 5. DEVELOPMENT OF AN INTELLIGENT SOFTWARE PACKAGE

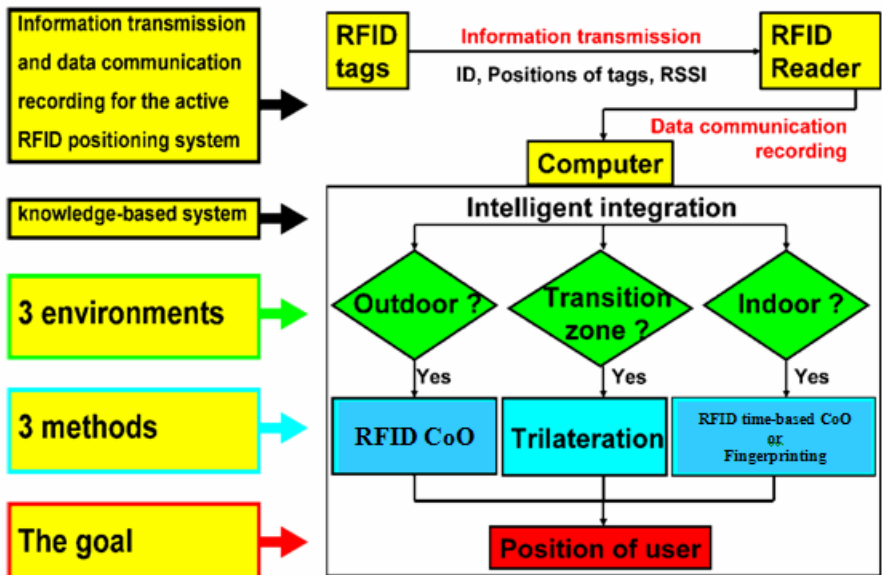
As presented in the introduction and in section 2, three different methods using RFID have been investigated and employed for positioning in indoor and urban outdoor environments, i.e., cell-based positioning (RFID CoO and RFID time-based CoO), trilateration and RFID location fingerprinting. The conducted tests demonstrate that these three different RFID positioning methods are quite appropriate for positioning in different environments such as an urban and indoor environment and a transition zone between these two. When the user walks from one environment to another, however, the method of positioning cannot be switched automatically. In other words, currently the corresponding software package of the positioning methods has to be selected manually when the environments change. In this section, a proposed concept is introduced for an intelligent knowledge-based software environment for continuous positioning in complex environments.

As mentioned above, the three different positioning methods are environment specific. For continuous positioning in complex environments, these three methods should be combined and integrated into one software package. In addition, the system should be able to automatically identify the type of environment

encountered by the user at this time point. This requires an intelligent integration of these three methods by a knowledge-based system (Fu and Retscher, 2008).

Figure 5 shows a preliminary concept for such an intelligent integration. The main focus is to develop an intelligent software environment. The software should support capturing the measurements from the employed sensors in real-time and processing the measured data within the required time. At the same time, the software should identify the current location environment and start the corresponding method of positioning automatically. Finally, the software should have a user friendly interface. With such a software and the knowledge-based system, continuous positioning in a complex environment could be carried out automatically. We propose to use fuzzy logic for the development of the intelligent software package. By formulating a number of conditions the selection of the suitable RFID positioning method can be performed. Then the membership functions of the fuzzy system form the knowledge-based system.

Figure 5 - Intelligent concept for the selection of the RFID positioning method depending on the environment of the pedestrian user.



## 6. CONCLUSIONS AND OUTLOOK

This paper addresses the investigation of different methods and algorithms for positioning using low-cost active RFID and INS for urban and indoor

environments. For the positioning using active RFID totally three different methods have been developed and investigated, i.e., cell-based positioning, trilateration using ranges to the surrounding RFID transponders (so-called tags) deduced from received signal strength measurements and RFID location fingerprinting.

The cell-based positioning is an algorithm to determine the location of the user in a cell around the RFID tag with a size defined by the maximum range of the RFID signals. The achievable positioning accuracies depend on the size of the cell, i.e., up to 20 m using our long range RFID equipment. Therefore, this method is only well suited for areas where accuracy is not that important, such as urban outdoor environment. However, the accuracy can be improved using a self developed algorithm that investigates the contribution of the measured signal strength around the RFID tag. This approach is called time-based Cell of Origin (CoO) and is introduced in this paper. The test results showed that the accuracy of positioning using time-based CoO is in the range of 1.30 m.

Trilateration can be employed if the ranges to several tags are determined and are used for intersection. The range from the antenna of the reader to the antenna of the tag is deduced from the conversion of signal power levels into distances. Strategies for the conversion of the signal strength measurements into distances are distinguished between indoor and urban outdoor environment. Using trilateration usually positioning accuracies on the one to a few meters level can be achieved.

For indoor environments also the use of RFID location fingerprinting was investigated. For the creation of the database in RFID location fingerprinting interpolation methods can be used, in order to achieve a further improvement of the positioning accuracy. The test of positioning using location fingerprinting showed that positioning accuracy below 1.00 m could be achieved.

Experiments have been carried out using the three methods of RFID positioning. In general, the experiments showed these three methods are appropriate for locating the user with different positioning accuracies, i.e., lower positioning accuracies in outdoor environment using cell-based positioning and higher positioning accuracies in indoor environments with trilateration and fingerprinting. The positioning is restricted, however, to areas where at least one RFID signal can be detected. If there is lack of coverage of signals of the RFID tags, the RFID reader will lose its orientation. In order to overcome these shortages we propose to integrate a low-cost Inertial Navigation System (INS) in addition.

In the project, a low-cost INS from Xsens, the MTi, has been employed. For calculating the positions from the measured data of the sensor the strapdown mechanization is used. Furthermore, a time-varying Kalman filter is employed to correct the position and acceleration resulted from the strapdown mechanization. RFID cell-based positioning is utilized to determine the current position of the user, when the RFID reader detects a signal from an RFID tag in the surrounding environment. The determined position will be needed to update and correct the



trajectory calculated by INS, since the INS components produce small measurement errors that accumulate over time and cause drift errors.

The above concept has been implemented and tested in a real world environment. For the combined positioning of RFID and INS an accuracy of around 1.00 m for continuous position determination can be achieved using our approach. From this result, it can be concluded that our approach using an integrated RFID cell-based and INS positioning with a time data capture tool is suitable for continuous position determination of a mobile user in challenging indoor environments.

## ACKNOWLEDGEMENTS

The research work presented in this paper is fully supported by the FWF Project “Ubiquitous Cartography for Pedestrian Navigation UCPNAVI” (Project No. P19210-N15) of the Austrian Science Fund (FWF Fonds zur Förderung wissenschaftlicher Forschung).

## REFERENCES

- BARBOUR, N.M. 2001. MEMS for Navigation – a Survey. In: Papers presented at the Institute of Navigation National Technical Meeting. Long Beach, CA, January 22-24, 2001.
- BROWN, R. G., HWANG, P. Y. C.. *Introduction to Random Signals and Applied Kalman Filtering*. John Wiley & Sons, New York, 3<sup>rd</sup> edition, 1997, 484 pp.
- FU, Q. Active RFID for Positioning Using Trilateration and Location Fingerprinting Based on RSSI. In: Papers presented at the ION GNSS Conference, September 16-19, 2008, Savannah, Georgia, USA, CD-Rom Proceedings, 14 pgs.
- FU, Q., RETSCHER, G. Using RFID Technology in Pedestrian Navigation for Information Transmission and Data Communication Recording. In: Papers presented at the Junior Scientist Conference, November 16-18, 2008, Vienna, Austria, 2 pgs.
- FU, Q., RETSCHER, G. Another Look Indoors – GPS + RFID. *GPS World*, 20(3), 2009a, pp. 40-43.
- FU, Q., RETSCHER, G. Active RFID Trilateration and Location Fingerprinting Based on RSSI for Pedestrian Navigation. *The Journal of Navigation*, 62(2), pp., 2009b. 323-340.
- GABAGLIO, V. GPS/INS Integration for Pedestrian Navigation. PhD thesis at Ecole Polytechnique Federale de Lausanne, Switzerland. 2002.
- KAEMARUNGSI K. Design of Indoor Positioning Systems Based on Location Fingerprinting Technique, Dissertation, 2005. University of Pittsburgh, see <http://etd.library.pitt.edu/ETD/available/etd02232005235903/unrestricted/dissertation28Feb05.pdf> (Last accessed: November 2009).

- LAWRENCE, A. *Modern Inertial Technology*. in: Guidance and Control., Springer-Verlag. 2<sup>nd</sup> edition. New York, 1998. 268 pgs.
- RETSCHER G., MOSER E., VREDEVELD D., HEBERLING D., PAMP J. Performance and Accuracy Test of aWiFi Indoor Positioning System, *Journal of Applied Geodesy*, Vol. 1, No. 2, 2007. pp. 103-110.
- RETSCHER, G., FU, Q. GNSS, RFID and INS Integration for Pedestrian Navigation. In: Papers presented at the GPS/GNSS 2008 Conference, Tokyo, Japan, November 11-14, 2008, CD-Rom Proceedings, 10 pgs.
- SHUSTER, M.D. A survey of Attitude Representations. *Journal of Astronautical Sciences*, 41(4), 1993, pp. 437-517.
- TITTERTON, D.H., WESTON, J.L. Strapdown Inertial Navigation Technology. Institution of Engineering and Technology; 2<sup>nd</sup> revised edition, 2005.
- XSENS. MTi and MTx User Manual and Technical Documentation, Product Manual, Xsens Technologies B.V., The Netherlands. 2007.